How to Cite: Ramasamy, M., Velayutham, G., & Pitchaipillai, R. (2025). A Novel Mannich Based Metal II Complexes: Synthesis and Characterization of Magnetic, Conductivity and Antimicrobial Properties. *Eurasian Journal of Chemistry, 30, 1(117), 60–75.* https://doi.org/10.31489/2959-0663/1-25-5

Article

Received: 24 January 2025 | Revised: 3 March 2025 |
Accepted: 12 March 2025 | Published online: 26 March 2025

UDC 541.49; 544.18

https://doi.org/10.31489/2959-0663/1-25-5

Manimegalai Ramasamy[1], Gurunathan Velayutham[2], Ramar Pitchaipillai[1*]

[1]PG and Research Department of Chemistry, Government Arts College, Bharathidasan University, Ariyalur, Tamilnadu, India;
[2]Research Department of Chemistry, Bishop Heber College, Bharathidasan University, Tiruchirappalli District, Tamilnadu, India
*(*Corresponding author's e-mail: drsairam202110@gmail.com)*

A Novel Mannich Based Metal II Complexes: Synthesis and Characterization of Magnetic, Conductivity and Antimicrobial Properties

A novel Mannich base (2R,9R)-2-((S)-((2-aminoethyl)amino)(2-hydroxyphenyl)methyl)-6-hydroxy-9-phenyl-2,3,4,9-tetrahydro-1H-xanthen-1-one (LI), composed from xanthene, salicylaldehyde, and ethylenediamine, was employed to synthesize unique complexes of Ni(II), Mn(II), Cr(II), Co(II), and Cu(II). The structural characteristics of the complexes were determined by studying microanalytical findings and using analytical methods such as EPR, FT-IR, ^{1}H & ^{13}C NMR, and UV-visible spectroscopy. The electronic spectra of the complexes suggested that the metal ion is fenced with octahedral structure. The molar conductivity of the metal chelates in DMSO was shown in the range of 18–28 $\Omega^{-1}mol^{-1}cm^{2}$. The EPR studies of the copper complex dissolved in dimethyl sulfoxide (DMSO) was obtained at temperature of 300 K, and its unique characteristics were analysed. The antimicrobial potential of the ligand and its complexes has been thoroughly examined towards *K. pneumaniae, S. aureus, P. aeruginosa, E. coli, C. albicans, C. neoformans, M. audouinii, A. niger* microorganisms. Experimental results have demonstrated that all of the complexes exhibit substantial antimicrobial action when related to both the unbound ligand and the standard. Furthermore, the validity of the biological research was verified through molecular docking antifungal and antibacterial tests. Overall, the obtained results confirm the multidirectional antimicrobial efficacy of the new Mannich base complexes and demonstrate their high pharmaceutical potential for further studies.

Keywords: Antimicrobial activity, Docking, Grindstone, Ligands, Mannich base, Metal complexes, Xanthene

Introduction

The emergence of antimicrobial resistance has evolved into a major worldwide health crisis, threatening to revert mortality rates to those observed in the pre-antibiotic era. Recent research by Murray et al. indicated that bacterial antimicrobial resistance was responsible for approximately 1.27 million fatalities in 2019 [1–3]. The alarming statistics are partly attributable to the incorrect and indiscriminate use of antibiotics, inadequate infection and disease prevention measures, and unequal access to quality, inexpensive medication [4]. As a result, bacteria have evolved several resistance mechanisms against nearly all medicines available today, jeopardizing the continuation of the 80-year "era of antibiotics". Examples of both innate and derived mechanisms of drug resistance in bacteria encompass target protection, alteration of target sites, enzymatic inactivation of antibiotics, active efflux, reduced inflow, and biofilm formation [5]. Microbial infestation refers to the process in which microbes, which include bacteria, viruses, and fungi, invade a living thing, replicate within it, and communicate with the host tissue [6]. These pathogens provide a significant public hazard to infections related to healthcare and are accountable for the mainstream of diseases in hospitals, leading to increased death and load on world health systems [7]. Specifically, metal complexes with heterocyclic ligands have a dominant role in medicinal chemistry due to its broad spectrum of characteristics [8–12]. Transition metal complexes are regarded as highly effective metallo-drugs for remedying the hazards posed by microorganisms [13, 14].

The production of heterocycles containing oxygen and nitrogen has long been a of great interest in organic chemistry. These compounds are often found in the fields of drug design, medical and pharmaceutical, and materials science [15–17]. Chromene and its analogues, specifically 2-amino-4H-chromene and 2H-chromene-2-one [6, 18], are a significant group of oxygen-containing heterocycles. These compounds incorporate a cyano moiety at the C-3 location which provides the possibility of being utilized in the dealing of several illnesses comprising psoriatic arthritis, rheumatoid arthritis, cancer therapy, Alzheimer's disease, Huntington's disease, Parkinson's disease, and amyotrophic lateral sclerosis [19–22]. They commonly occur

in the fundamental structure of numerous herbal remedies and manufactured potential medicines. They are of great importance in medicinal chemistry due to its significant pharmacological functions, which include antifungal, antioxidant, antiproliferative, antimicrobial, antitumor, anticoagulant, and anti-allergic properties (Fig. 1) [23–27]. In recent decades, various material science applications like laser dyes, optical brighteners, and fluorescence markers have been developed [28–30]. In addition, they find use in beauty products, recyclable agrochemicals, colourants, and other areas [31–33].

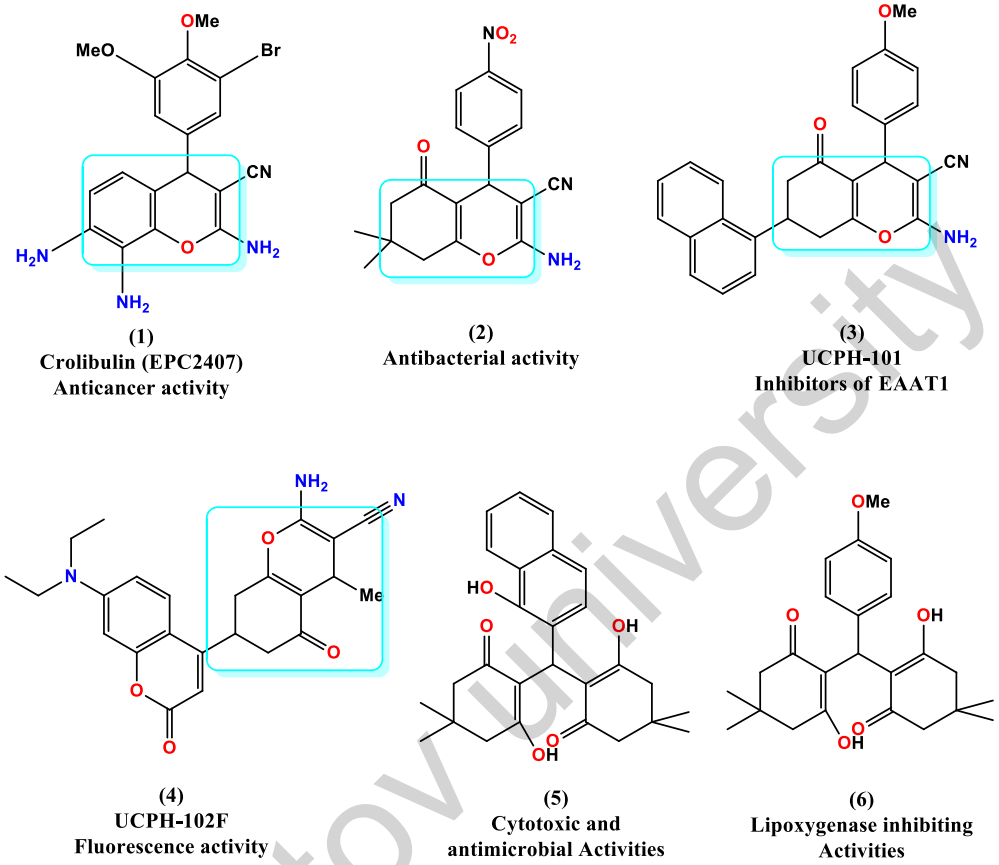

Figure 1. 2-amino-4*H*-chromene (1–4) and tetraketones (5–6) with probable optoelectronic and medicinal uses

Mannich transformations provide an unswerving and effectual method for synthesising β-amino carbonyl substances, which are important in the manufacturing of various medicines, synthetic materials, and natural substances [34–36]. These methods are used to produce distinctive carbon-carbon bonds in the creation of nitrogen-bearing substances in organic synthesis [37, 38]. Mannich bases play a crucial role in medicinal chemistry due to their ability to form substantial 3d-metal complexes with unique therapeutic value [39, 40]. The progress of innovative catalytic approaches for the fabrication of Mannich bases is crucial in the field of synthetic chemistry. Several scholars have documented Mannich derivatives having catalysis action [41–43]. The complexation behaviour of Mannich analogues was crucial in advancing the field of inorganic chemistry [44].

Metal complexes with heterocyclic ligands demonstrate a wide range of actions, including antimicrobial, antibacterial, anti-inflammatory, antioxidant, antitumor, antiviral, antidiabetic, antifungal, antimalarial, anticonvulsant, anticancer, antiamoebic, antiproliferative, and anti-HIV properties [45–49]. However, the production of metal complexes mediated by Xanthene is not well documented. Consequently, this study was conducted on the Mannich base ligand (L1), emphasizing its biological relevance. The current investigation was undertaken on the Mannich base ligand (L1), taking into consideration its biological significance. The compound was produced through the condensation reaction of xanthene, salicylaldehyde, and ethylenediamine. The Mannich base that was synthesised was subsequently coordinated with chlorides of Mn(II), Co(II), Ni(II), Cr(II), and Cu(II). The synthesised compounds were characterised using several spectroscopic and chemical approaches, and their antimicrobial capabilities were assessed.

Experimental

Chemistry

All the substances and solvents used were of extremely pure grade (Analar grade, A.R.) and obtained from Sigma-Aldrich. The identification of complexes was achieved by acquiring FT-IR spectra of the ligand and complexes within the frequency array of 400–4000 cm^{-1}. This was done by KBr pellets and an Agilent Resolutions spectroscopy. The absorbance spectra of the ligand (**L1**) and associated complexes (**1-5**) were acquired using a Shimadzu UV mini-1240 UV spectroscopy in the wavelength range of 300–1100 nm to determine the potential electronic transitions.

Synthesis of Ligand (L1)

A blend of salicylaldehyde (2.4 mL, 0.02 mol), xanthene (5.85 g, 0.02 mol), and ethylenediamine (1.2 mL, 0.02 mol) were pulverised together in a mortar for a duration of 10 minutes through grindstone chemistry technique. The progression of the reaction was monitored by thin-layer chromatography (TLC). Once the chemical process designated by TLC was finished, the resulting mixture was placed in crushed ice. The raw product was filtered and dehydrated. To purify the ligand, it was recrystallized using hot ethanol. The production of ligand (**L1**) is shown in Figure 2.

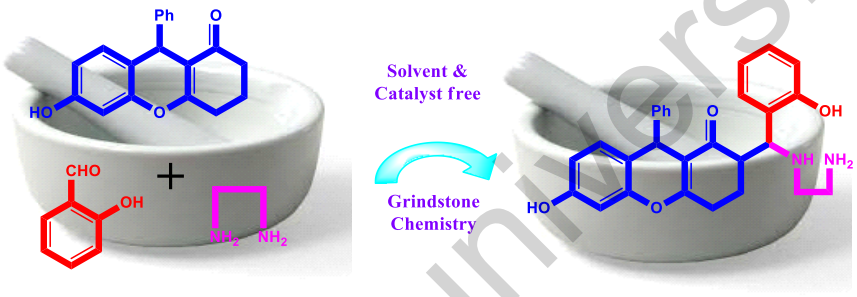

Figure 2. Preparation of ligand (**L1**)

*Synthesis of Metal Complexes (**1-5**)*

Under reflux, a hot ethanolic solution containing (0.02 mol) of ligand **L1** was gradually combined with (0.01 mol) of metal chlorides in a hot ethanolic solution with continuous stirring. After the final reaction stage, the reaction mixture was left at ambient temperature to evaporate. The impure metal complex was refined by column chromatography employing a combination of elutant DCM:CH_3CN:CH_3OH (2:3:5 v/v) over silica gel. Metal complexes (**1–5**) were synthesised as shown in Figure 3.

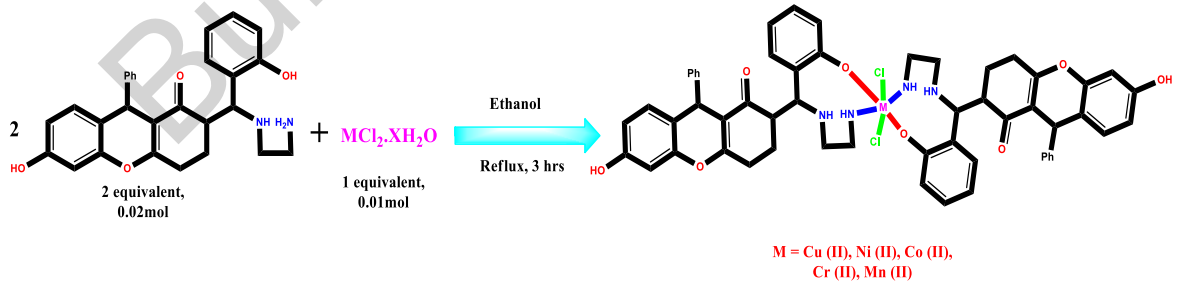

Figure 3. Preparation of metal complexes (**1–5**)

Solubility Measurements

The solubility of the ligand and complex in protic and aprotic solvents was determined. Water, alcohol, acetone, chloroform and dimethylsulfoxide were used as solvents. Based on the findings of the solubility evaluations more investigations were constructed.

Magnetic Susceptibility Measurement

The combination of magnetic susceptibility investigations and absorbance spectra can be employed to determine the structure of the complex. Magnetic characteristics can be utilised to ascertain the stereochemistry of a metal ion complex with d^5, d^6, d^7, d^8, or d^9 electron configuration, specifically whether it adopts a tetrahedral, square planar, or octahedral arrangement. Additionally, these parameters can indicate if the complex is spin-free or spin-paired. The magnetic properties of the metal atoms in the current complexes were inspected utilizing a Gouy magnetic balance to identify the most favourable magnetic moment for each atom at ambient temperature. The Gouy tube was standardized with mercury(II) tetrathiocyanatocobaltate(II), also known as $Hg[Co(SCN)_4]$. The diamagnetic modifications for several atomic and structural components were determined using Pascal's coefficients. The effective magnetic moments ($\mu_{eff.}$) were determined based on the molar magnetic susceptibilities (M_{corr}) of the complexes employing Curie's formula, $\mu_{eff} = 2.84\ [M_{corr}\ T]^{1/2}$ B.M., where T represents the absolute temperature at which the measurements were made. The number of metal ions with unpaired electrons, 'n', can be calculated by analysing its effective magnetic moment, eff. The equation $\mu S = [n\ (n+2)]^{½}$ demonstrates the contribution of the electronic spin effect (S) to the moment.

Antibacterial Effect

The ligand (**L1**) and its complexes (**1–5**) were subjected to *in vitro* antibacterial evaluations towards *P. aeruginosa* (PA14), *K. pneumoniae* (342), *E. coli* (k12), and *S. aureus* (PS80) bacteria using the Kirby Bauer Disc diffusion technique [50]. Ciprofloxacin's antibacterial effect was used as a standard. The bacterial specimens were grown on petri plates containing nutrient agar medium. The test samples were made up of DMSO and placed inside a filter paper disc with a width of 5 mm and a width of 1 mm. Following a 24-hour period, the breadth of the inhibitory zone [51, 52] around each disc was assessed to determine its antibacterial effectiveness. The discs were then positioned on the pre-existing plates and incubated at a temperature of 37 °C. The minimum inhibitory concentrations (MIC) were employed to indicate the antibacterial effectiveness of ligand (**L1**) and its associated complexes (**1–5**).

Antifungal Action

The antifungal effect of ligand (**L1**) and its complexes (**1–5**) was evaluated using the regular disc-agar diffusion approach [53, 54]. The antifungal activity was tested using *A. niger* (ATCC20611), *C. neoformans* (H99), *C. albicans* (WO-1), and *M. audouinii* (ATCC-10216) species. The materials underwent sterilisation by filtration through 0.22 m Millipore filters upon their dissolution in 10 % DMSO to achieve a target dosage of 30 mg/mL. Subsequently, antifungal tests were conducted using the disc diffusion method. A solution comprising 100 litres and 10^4 spores/mL of fungi was disseminated across PDA medium. The 6 mm diameter discs were subjected to a treatment of 10 mL of the samples, with each disc weighing 300 g. Subsequently, the discs were placed on the agar that was contaminated. The conventional medication prescribed was clotrimazole. Negative controls were prepared using a 10 % solution of dimethyl sulfoxide (DMSO). The fungal specimens were cultured at 37 °C for 72 hours on inoculation plates. Plant-associated fungi were cultivated at a temperature of 27 °C. The antifungal effectiveness was assessed by gauging the ZOI towards the investigated microorganisms. Every experiment in the present investigation was performed three times.

Determination of MIC

The microbial cultures often used to make 0.5 McFarland were cultured overnight at 37 °C. Each culture was inoculated in aseptic conditions with 1 mL of the specific bacterial culture (around 10^8 CFU/mL) from a minimum of a 10 mL tube nutritional broth medium. In sterile deionized water, five dilutions of ligand (L1), metal complexes (**1–5**) (100, 75, 50, and 25 mg/mL) were made, as well as a blank sample (without ligand (**L1**), metal complexes (**1–5**)). All isolate evaluations were carried out in triplicate. The implanted tubes were maintained at 37 °C overnight. During the cultivation period, the perceived turbidity in every tube was evaluated. The MIC is demonstrated as the lowermost concentration of the observed strain without turbulence.

Molecular Docking

The relationship and binding mechanism amongst the ligand (**L1**), complexes (**1–5**), and the Mevalonate 5-diphosphate decarboxylase (PDB ID: 1FI4) and Topimerase II DNA gyrase B (PDB ID: 1KZN) proteins were examined through docking analyses using Autodock vina 1.1.2 software [55]. The crystal structures of Mevalonate 5-diphosphate decarboxylase (PDB ID: 1FI4) and Topimerase II DNA gyrase B (PDB

ID: 1KZN) were gotten from the Protein Data Bank for the purpose of assessing their antimicrobial and capabilities. The 3D conformation of ligand **L1** and its complexes (**1–5**) were obtained using ChemBio Office suite software. The required inputs for docking process were generated through the AutoDock Tools 1.5.6 software. The grid dimensions for the 1KZN receptor was determined to have a centre position at x-coordinate 18.839, y-coordinate 26.702, and z-coordinate 37.939. The parameters of the grid are as follows: size_x = 22, size_y = 20, and size_z = 20. The distance between each point on the grid is 1.0 Å. The grid dimensions for the 1FI4 receptor were determined to have a centre position of x: 21.935, y: 57.745, and z: 20.018, with size of x: 24, y: 22, and z: 24, with a spacing of 1.0 Å. The exhaustiveness score was assigned a numerical value of 8. The remaining settings were fixed to their actual parameters for Vina docking and were not specified. The substance with the lowest binding score is considered the potential compound. The docking results were evaluated with the Discovery Studio 2019 application.

Statistical Analysis

Data are presented as mean ± standard error (SEM). All variables were analyzed for statistics by one-way ANOVA subsequently by Tukey's post-hoc comparison test. $P < 0.05$ was considered statistically significant.

Results and Discussion

Physical Data and Solubility

Table 1 displays the physio-chemical properties and solubility of the ligand (**L1**) and its complexes (**1–5**). Solubility experiments indicate that each of the ligand (**L1**) and the metal complexes (**1–5**) exhibit higher solubility in aprotic solvents as opposed to protic solvents.

Table 1

Physical data and solubility of the metal complexes (1–5) and ligand (L1)

Compound	Colour	Melting point (°C)	Solubility			
			Chloroform	Water	DMSO	Ethanol
Ligand (L1)	Yellow	164	Sparingly soluble	Insoluble	Soluble	Soluble
Copper complex (1)	Blue	186	Insoluble	Insoluble	Soluble	Insoluble
Nickel complex (2)	Green	194	Insoluble	Insoluble	Soluble	Sparingly soluble
Cobalt complex (3)	Pale brown	206	Insoluble	Insoluble	Soluble	Insoluble
Chromium complex (4)	Dark brown	182	Partially soluble	Insoluble	Soluble	Insoluble
Manganese complex (5)	Black	234	Insoluble	Insoluble	Soluble	Insoluble

Spectral Data of Ligand (L1)

(2R,9R)-2-((S)-((2-aminoethyl)amino)(2-hydroxyphenyl)methyl)-6-hydroxy-9-phenyl-2,3,4,9-tetrahydro-1H-xanthen-1-one (L1)

Yellow solid; Mw: 456.53; mf: $C_{28}H_{28}N_2O_4$; mp: 165 °C; IR (cm^{-1}, KBr) ν_{max}: 3420 (–OH), 3230 (–NH), 1640 (–C=O), 1230 (–C–N–C); ^{1}H NMR (300 MHz, $CDCl_3$) δ 10.38 (2H, s, OH), 8.08 (1H, s, NH), 7.12–6.90 (4H, m, Ph–OH), 7.33–7.23 (5H, m, Ar–H), 6.89–6.19 (3H, m, Ph–OH), 6.25 (2H, s, NH_2), 4.74 (1H, s, –CH–Ph), 4.12 (1H, d, J = 1.7 Hz, CH-Ph), 2.96–1.27 (5H, m, CHD), 2.77 (2H, t, J = 2.8 Hz, $–CH_2$), 2.61 (2H, t, J = 2.8 Hz, $–CH_2$); ^{13}C NMR (300 MHz, $CDCl_3$) δ 198.6 (1C, C=O), 164.8 (1C, -C=C), 162.9, 154.5, 130.3, 112.9, 110.6, 100.1 (6C, Ar ring), 147.6, 129.2, 128.2, 126.2 (6C, Ph ring), 155.2, 127.7, 127.3, 121.1, 115.7 (6C, Ph ring), 109.7 (1C, –C=C), 57.0 (1C, –C–C–Ph), 51.1 (1C, –C–NH), 48.9 (1C, $–CH_2–$NH), 41.3 (1C, $–CH_2–NH_2$), 39.9 (1C, –CH–Ar), 26.3 (1C, CH_2), 12.6 (1C, CH_2); EI-MS: m/z 457.21 (M^+, 30 %); Elemental studies: Anal. Calcd (Found): C, 73.66 (73.62); H, 6.18 (6.20); N, 6.14 (6.16) %.

Magnetic and Conductivity Properties

The solubility of the newly synthesised metal complex was assessed in several solvents. The molar conductivity in DMSO was determined by utilising a cell constant that was standardised towards a 0.1 M KCl solution. The measurement was performed using the Equiptronics electronic conductivity meter (Model EQ-660). The complexes' neutral (non-electrolytic) character was confirmed by assessing the conductivity of

a 10^{-3} M solutions for every complex in DMSO. The mixed ligand complexes (**1–5**) exhibited a molar conductivity of 18–28 $\Omega^{-1}mol^{-1}cm^2$. The conductivity studies revealed that the chloride ions form complexes with metal ions, signifying that they act as ligands instead of independent ions. The arrangement of the synthesised complexes may be influenced by the stoichiometric ratios (1:2) and the kinds of electrolytes employed in the conductivity testing. Table 2 presents the conductivity and magnetic properties of metallic complexes (**1–5**).

Table 2

Conductivity and magnetic properties of metal complexes (1–5) with ligand (L1)

S. No	Compounds	Conductivity ($\Omega^{-1}mol^{-1}cm^2$)	Magnetic Susceptibility (μ_{eff}. B.M)
1.	Copper complex (1)	18	2.23
2.	Nickel complex (2)	26	3.54
3.	Cobalt complex (3)	23	5.23
4.	Chromium complex (4)	24	4.60
5.	Manganese complex (5)	28	5.14

NMR Spectral Studies of Ligand (L1)

In the ^{1}H NMR spectra of the Mannich base ligand (**L1**) being studied (Fig. S1, *a*). The methylene protons associated with the amine hydrogen atoms of the ethylenediamine and salicylaldehyde are observed as a peak at 4.74 ppm, while the hydroxyl protons appear at 10.38 ppm. The aromatic hydrogens exhibit a multiplet at 7.12–6.90 ppm. The lack of a signal corresponding to the proton of the secondary amine $–NH_2$, which was eliminated during the Mannich process, provides more evidence for the creation of the ligand. In the ^{13}C NMR spectra of the Mannich base ligand (**L1**) being studied, the peak at 198.6 and 164.8 ppm resemble to the –C=O and –C=C atoms of the xanthene group, respectively. The carbon atoms of the aromatic rings exhibited peaks at 162.0–100.1 ppm (Fig. S1, *b*). The appearance of a peak at 39.9 ppm indicates that the $–CH_2$ moiety is connected to the amine hydrogens of the ethylenediamine and salicylaldehyde.

Mass Spectral Studies of Ligand (L1)

The mass spectra of the studied Mannich base ligand (**L1**) is shown in Figure 4. The mass of ligand (**L1**) was determined to be 456.53 through observation, and this was further validated by mass spectral tests, which showed a mass-to-charge ratio (m/z) of 457.23. The molecular ion peak was detected at a m/z of 380.44. The other fragmentation peaks seen had m/z of 412.03, 291.32, 225.26 and 209.26, accordingly. The fragmentation pattern of ligand (L1) was depicted in Figure 5.

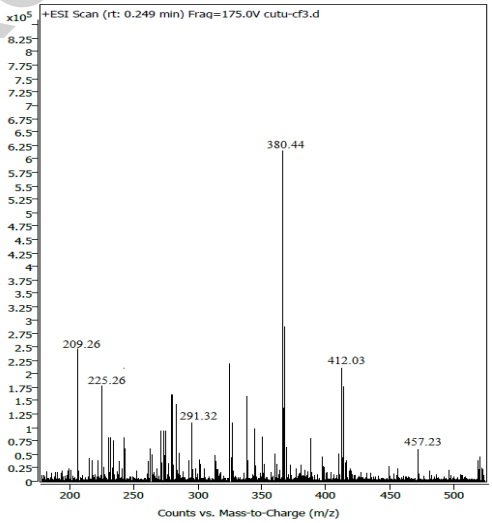

Figure 4. Mass spectra of ligand (L1)

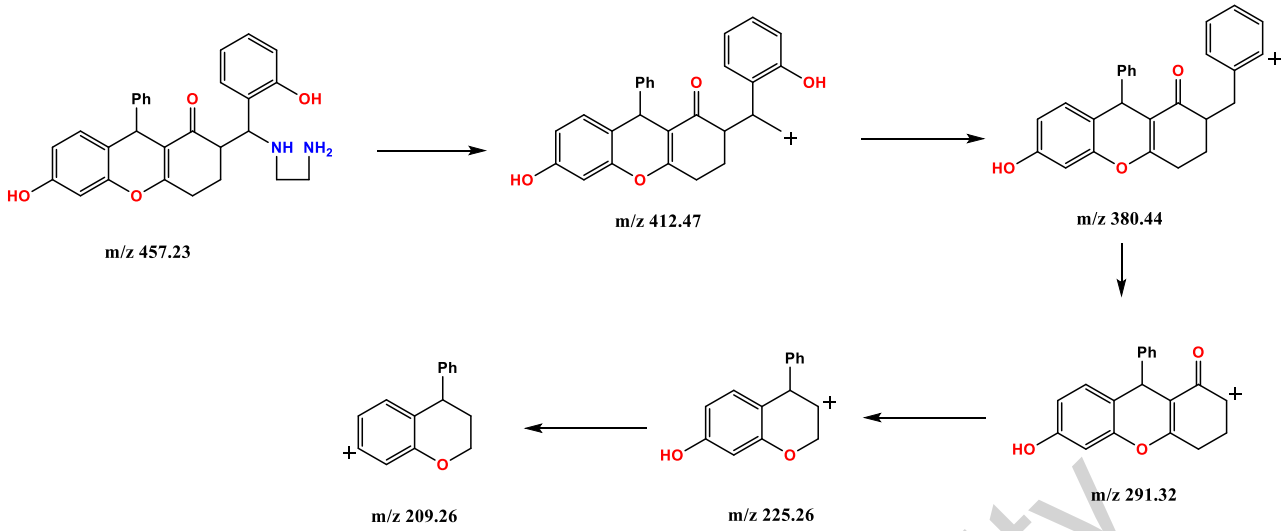

Figure 5. Mass spectral fragmentation types of Ligand (L1)

IR Spectra

A notable discovery in the ligand FT-IR spectra (Fig. 6*a*) displayed a prominent band at 3446 and 3145 cm^{-1}, which can be ascribed to the *v*OH and the NH amine molecule [56, 57]. The N–H and O–H bands exhibited a shift towards lower frequency in all of the complexes (Figs 6*b–f*), demonstrating that the hydroxyl oxygen and amine nitrogen were tangled in coordination with the metal ions. The formation of metal complexes (**1–5**) is indicated by the emergence of a distinct peak at a wavelength of 760–752 cm^{-1}, which resembles to the M–O bond [58]. The M–Cl bond is shown by the emergence of a distinct peak in the spectral array of 546–514 cm^{-1}. Table 3 presents the IR spectral information for ligand **L1** and complexes **1–5**.

Table 3

FT-IR studies of complexes (1-5) and the ligand (L1)

Compound	IR stretching frequency (cm^{-1})			
	–OH	–NH	M–O	M–Cl
Ligand (L1)	3446	3145	–	–
Copper complex (1)	3423	2938	760	514
Nickel complex (2)	3478	3062	756	546
Cobalt complex (3)	3437	3058	752	542
Chromium complex (4)	3427	2939	756	523
Manganese complex (5)	3441	2940	752	528

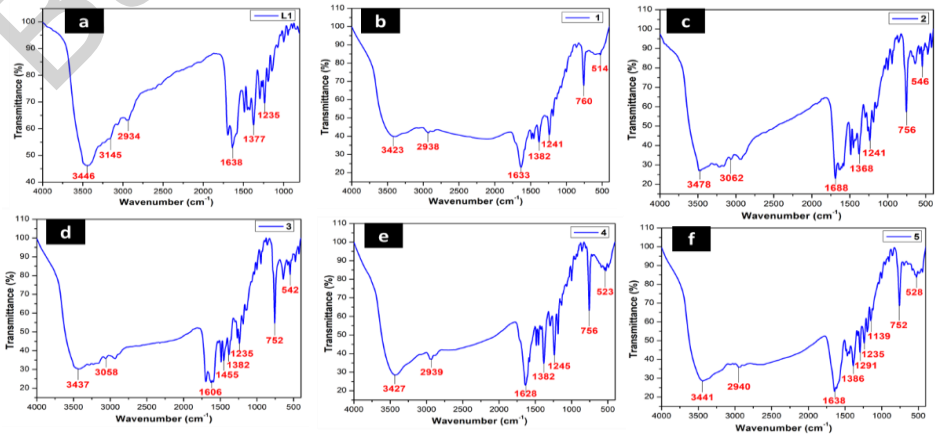

Figure 6. FT-IR spectra of (*a*) Ligand **L1** (*b*) Copper complex **1** (*c*) Nickel complex **2** (*d*) Cobalt complex **3** (*e*) Chromium complex **4** (*f*) Manganese complex **5**

UV-Visible studies

The UV-Vis spectra of ligand (**L1**) displayed two absorption maxima in the area of 219 and 266 nm, which can be attributed to π–π* and *n*–π* shifts separately (Fig. 7*a*). The spectra of the complexes in DMSO solution revealed three distinct peaks. The intra-ligand shifts were identified by two distinct bands observed at 272–278 nm and 245–258 nm. The presence of the complex was described by the peak observed in the 343–332 nm area, which is recognized to the ligand-to-metal charge transfer (LMCT) shifts (Figs 7*b*-*f*).

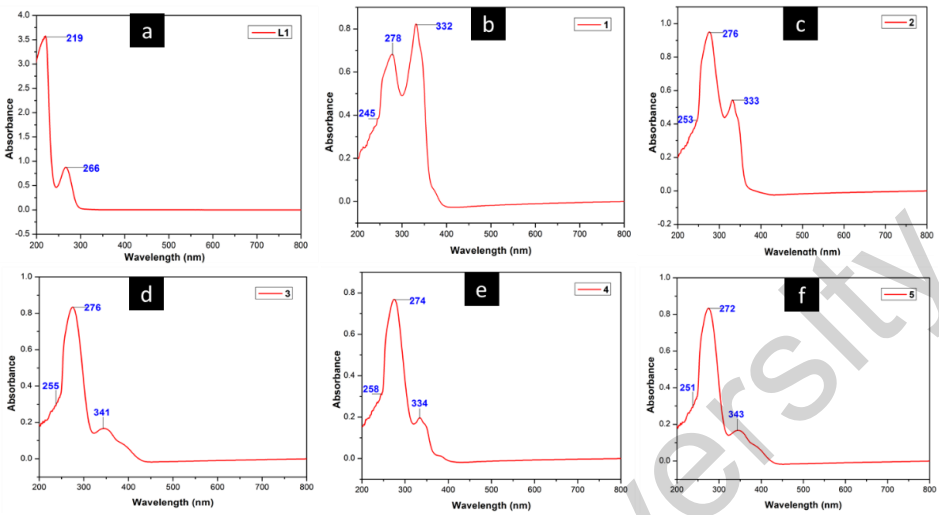

Figure 7. UV-Vis spectra of (*a*) Ligand L1 (*b*) Copper complex 1 (*c*) Nickel complex 2 (*d*) Cobalt complex 3 (*e*) Chromium complex 4 (*f*) Manganese complex 5

EPR Spectra

EPR spectrum study can provide insights on the formation of ligand-metal bonds and the distribution of unpaired and paired electrons. Copper (II) complexes exhibit distinct characteristics in coordination chemistry, displaying several geometries including square pyramidal, octahedral, square planar, and tetrahedral, which can be differentiated by EPR spectra. The EPR parameters $g_{\perp}$, g_{avg}, $g_{\parallel}$, and G are used to determine whether a chemical has an octahedral or tetrahedral structure. The occurrence of an unpaired electron in the $d_{x^2-y^2}$ orbital is confirmed by the following criterion: the parallel g-value ($g_{\parallel}$) is larger than the perpendicular g-value ($g_{\perp}$), which is more than 2.0023. The $g_{\parallel}$ and $g_{\perp}$ values for the copper complex were measured to be 2.1465 and 2.0253, individually. The covalent character was denoted by a $g_{\parallel}$ value less than 2.3 and anionic character is represented by a $g_{\parallel}$ value greater than 2.3. It is evident that the $g_{\parallel}$ value (2.1465) is less than 2.3, suggesting that the molecule is covalent. Hathaway states that G values below four suggest a substantial interaction towards metal centres, while G values above four designate a minimum transfer of charge. In this example, the G value is 11.45, indicating that the charge transfer is minimum. The Cu(II) complex has distorted octahedral geometry, as indicated by its EPR properties. The EPR spectra of copper complex (**1**) are shown in Figure 8.

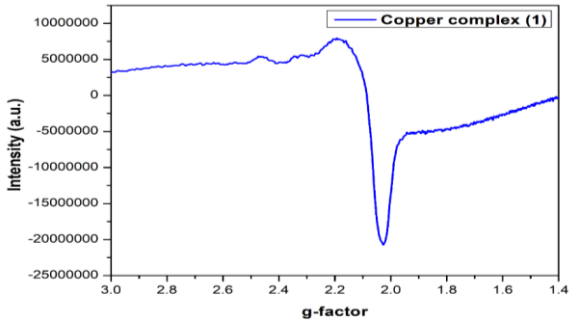

Figure 8. EPR spectra of copper complex **1**

Antibacterial Effect

The synthesised ligand (**L1**) and complexes (**1–5**) were evaluated for antibacterial properties. The ligand (**L1**) exhibited lower activity in comparison to the equivalent complexes (**1–5**). The examination was conducted within a regulated setting. Among the series of compounds (**1–5**), only complex **1** exhibited significant action (MIC = 2 mg/mL) towards *S. aureus*. The chromium complex **4** exhibited more activity towards *K. pneumoniae* compared to the control Ciprofloxacin, as seen by its lower MIC value of 4 mg/mL, in contrast to Ciprofloxacin's MIC value of 8 mg/mL. The cobalt complex 3 had higher activity towards *E.coli* related to the control Ciprofloxacin, as evidenced by its lower MIC value of 4 mg/mL, whereas Ciprofloxacin had a MIC value of 6 mg/mL. Complexes **1** (Cu(II)), **3** (Co(II)), and **4** (Cr(II)) exhibit remarkable activity when compared to complexes **1–5**. Janowska et al., reported the synthesis of metal complexes using heterocyclic Mannich base ligand and its excellent antibacterial action [59]. The outcomes are presented in Table 4 and Figure 9.

Table 4

Antibacterial effect of ligand (L1) and Complexes (1–5)

Compounds	MIC in mg/mL			
	K. pneumaniae	*S. aureus*	*P. aeruginosa*	*E. coli*
L1	16	32	32	16
1	12	2	8	10
2	28	8	8	8
3	14	10	4	4
4	4	6	4	12
5	16	12	4	8
Ciprofloxacin	8	4	2	6

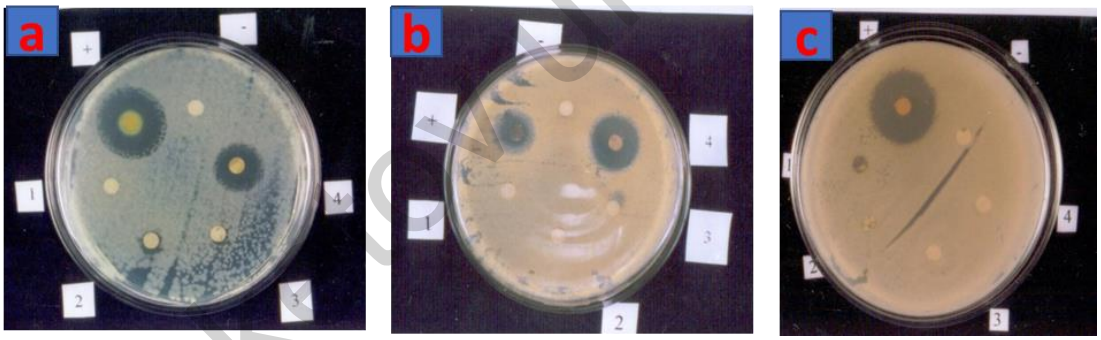

Figure 9. Antibacterial action of copper complex 1 in (*a*) *K. pneumaniae*, (*b*) *S. aureus*, (*c*) *E. coli*

Antifungal Activity

The study examined the antifungal effect of the obtained ligand (**L1**) and its complexes (**1–5**). Compared to similar complexes, the ligand (**L1**) exhibited low activity (**1–5**). The complex **1** in the sequence (**1-5**) had significant activity specifically towards *C. albicans*, having MIC of 4 mg/mL. The nickel complex **2** exhibited higher activity towards *C. neoformans* compared to the normal Clotrimazole. The MIC of the nickel complex **2** was 2 mg/mL, whereas the MIC of Clotrimazole was 4 mg/mL. The cobalt complex 3 exhibited a lower MIC of 8 mg/mL against *A. niger* compared to the normal Clotrimazole, which had an MIC of 12 mg/mL. Complex **1** (Cu II), complex **2** (Ni II), and complex **3** (Co II) exhibit significant activity in comparison to complexes (**1–5**). The antibacterial efficacy of the complexes is ascribed to the existence of heterorings and heteroatoms [60]. The antibacterial efficacy of the metal complexes tends to be superior to that of the ligand alone. This results from the extensive delocalization of the ligand's electronic orbitals throughout the metal complexes, hence diminishing the metal's polarity. This, in turn, enhances the lipophilicity of the complex, which ultimately leads to the occlusion of active binding sites of microbial enzymes [61]. The findings are summarised in Table 5 and Figure 10.

Table 5

Antifungal effect of ligand (L1) and complexes (1–5)

Compounds	MIC in mg/mL			
	C. albicans	*C. neoformans*	*M. audouinii*	*A. niger*
L1	14	26	16	10
1	04	08	12	16
2	12	02	10	24
3	10	16	12	08
4	12	11	10	14
5	14	11	08	15
Clotrimazole	08	04	10	12

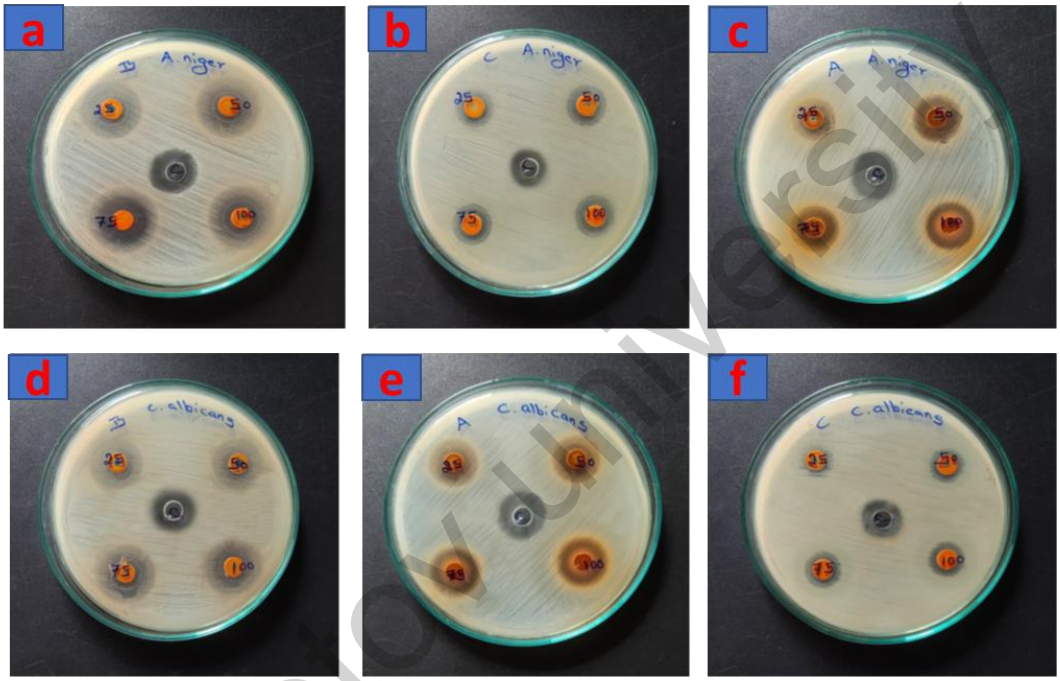

Figure 10. Antifungal action of (*a*) cobalt complex, (*b*) chromium complex, (*c*) Ligand **L1**, (*d*) copper complex, (*e*) cobalt complex, (*f*) chromium complex

Docking Studies

Docking studies were performed to have a deeper understanding of the potential mechanisms of biological processes. The anti-fungal protein mevalonate-5-diphosphatedecarboxylase (PDB ID: 1FI4) [62] which is accountable for isoprenoid/sterol production and the *E. coli* topoisomerase II DNA gyrase B (PDB ID: 1KZN) [63] were selected as protein targets for assessing antimicrobial action towards these species. The ligand **L1**, together with complexes (**1**–**5**) and the control substances Clotrimazole and Ciprofloxacin [64], were analysed for their docking interactions with receptors 1FI4 and 1KZN employing the Autodock Vina software. The complexes (**1**–**5**) exhibit higher binding affinities (–7.9, –6.2, –7.8, –7.7, –6.8 kcal/mol) compared to ligand **L1** (binding affinity: –5.3 kcal/mol) and control Ciprofloxacin (binding affinity: –6.0 kcal/mol) in complex with the 1KZN receptor. Hydrogen bonding significantly contributes to the reliability of protein-ligand interaction. The ideal bond length amongst the hydrogen-acceptor and hydrogen-donor atoms is less than 3.5 Å [65]. The hydrogen bond lengths between ligand **L1**, complexes (**1**–**5**), and control Ciprofloxacin were all below 3.5 Å in their respective proteins, which exhibited particularly high hydrogen bonding. The ligand **L1** establishes four hydrogen bonds with the protein 1KZN. The amino acids Glu42 (bond length: 2.90 Å), Asn46 (bond lengths: 2.43 and 2.50 Å), and Arg136 (bond length: 2.56 Å) participated in hydrogen bonding contacts. Hydrophobic contacts were mediated by the amino acids Glu50, Arg76, Gly77, Ile78, Pro79, Gly119, and Val120. Complex **3** establishes two Hydrogen bonds with the pro-

tein 1KZN. The amino acid residue Arg76 participated in a hydrogen bonding interaction, with bond lengths of 2.20 and 3.04 Å. Hydrophobic interactions were facilitated by the amino acids Asp49, Glu50, Ala53, and His95. Ciprofloxacin failed to create any hydrogen bonds with the protein 1KZN. Hydrophobic interactions occurred between each of the amino acids Asn46, Ala47, Glu50, Asp73, Ile78, and Ile90. Figures 11a–c illustrate the hydrophobic and hydrogen bonding relations between amino acids in the ligand **L1,** copper complex **(1),** Ciprofloxacin and 1KZN receptor. Figures S2–S5 illustrate the hydrophobic and hydrogen bonding relations between amino acids in the complexes (**2**–**5**) and 1KZN receptor. The complexes (**1**–**5**) exhibit higher binding affinities (–8.8, –8.0, –8.3, –7.0, –7.4 kcal/mol) compared to ligand **L1** (binding affinity: –6.2 kcal/mol) and control Clotrimazole with a binding affinity of (–6.7 kcal/mol) in the 1FI4 receptor, correspondingly. The ligand **L1** establishes six hydrogen bonds with the protein 1FI4. The amino acids Asn13, Ala119, Arg158, Asp201, Val206, and Ser208 were implicated in hydrogen bonding interactions, with bond lengths of 2.72 Å, 2.48 Å, 2.44 Å, 2.82 Å, 3.00 Å, and 2.05 Å, individually. Hydrophobic contacts were facilitated by the amino acid residues Ala15 and Asp302. Complex **2** establishes three hydrogen bonds with the target protein 1FI4. Hydrogen bonding interactions involving the amino acids Asn110 (with a bond length of 3.09 Å), Ser208 (with a bond length of 1.67 Å), and Ala303 (with a bond length of 1.82 Å). Hydrophobic relations were mediated by the amino acids Ala15, Ala119, Arg158, and Asp302. The control Clotrimazole molecule forms a single hydrogen bond with the target protein 1FI4. The amino acid Arg158, with a bond length of 5.83 Å, participated in a hydrogen bonding interaction. Hydrophobic contacts were facilitated by the amino acids Ala15, Lys18, Tyr19, Trp20, Ala119, Phe260, Asp302, and Ala303. Figures 12*a–c* depict the hydrophobic and hydrogen bonding contacts between amino acids in the 1FI4 protein and ligand **L1**, copper complex (**1**) and the control Clotrimazole. Figures S6–S9 depict the hydrophobic and hydrogen bonding contacts between amino acids in the 1FI4 protein and complexes (**2**–**5**). The results indicate that complexes (**1**–**5**) exhibit much higher inhibitory capacity compared to ligand **L1** and the control substances Clotrimazole and Ciprofloxacin in terms of antifungal and antibacterial properties. The findings were simplified and presented in Table 6 and Table 7.

Table 6

Docking results of ligand L1 and complexes (1–5) against protein 1KZN

Compounds	Binding score (kcal/mol)	No. of H-bonds	H-bonding residues
L1	–5.3	4	Glu42, Asn46, Arg136
1	–7.9	0	–
2	–6.2	0	–
3	–7.8	2	Arg76
4	–7.7	0	–
5	–6.8	0	–
Ciprofloxacin	–6.0	0	–

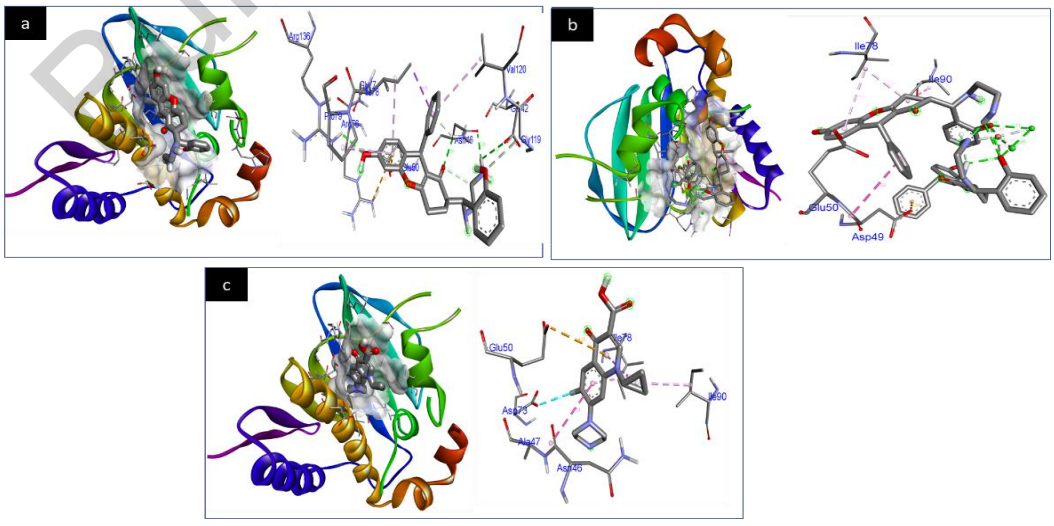

Figure 11. Interactions of ligand L1 (*a*), copper complex 1 (*b*), Ciprofloxacin (*c*) within the binding cavity of 1KZN

Table 7

Docking results of ligand L1 and complexes (1–5) against protein 1FI4

Compounds	Binding score (kcal/mol)	No. of H-bonds	H-bonding residues
L1	-6.2	6	Asn13, Ala119, Arg158, Asp201, Val206, Ser208
1	-8.8	1	Tyr19
2	-8.0	3	Asn110, Ser208, Ala303
3	-8.3	1	Leu17
4	-7.0	1	Asp302
5	-7.4	0	-
Clotrimazole	-6.7	1	Arg158

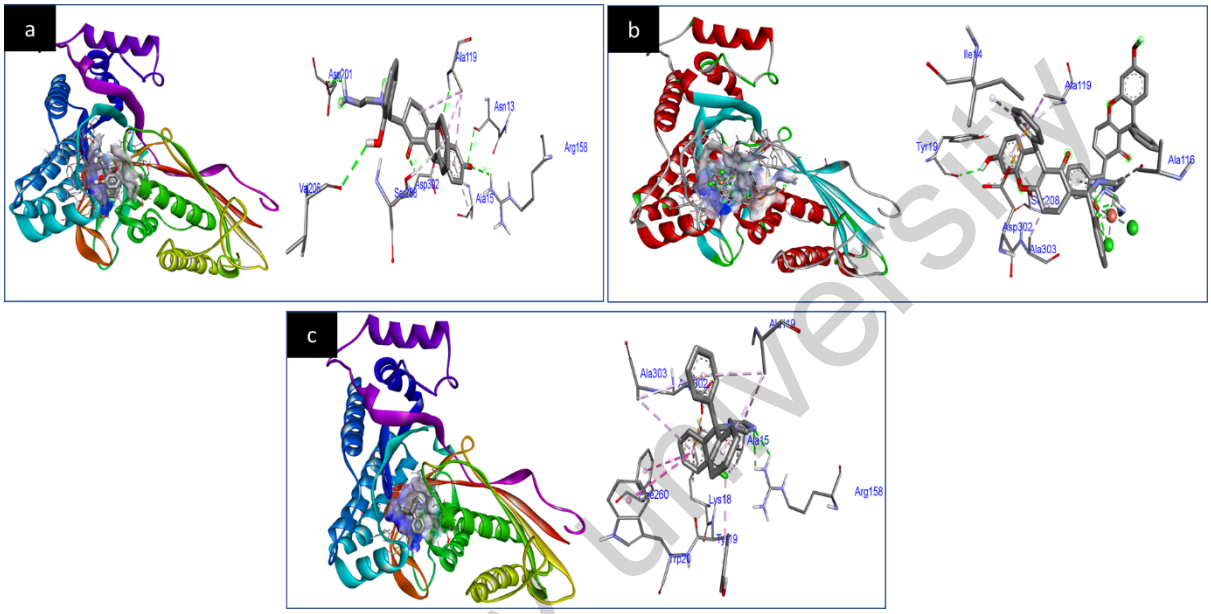

Figure 12. Interactions of ligand L1 (*a*), copper complex 1 (*b*), Clotrimazole (*c*) within the binding cavity of 1FI4

Conclusions

This study focusses on the coordination chemistry of a Mannich base ligand (2R,9R)-2-((S)-((2-aminoethyl)amino)(2-hydroxyphenyl)methyl)-6-hydroxy-9-phenyl-2,3,4,9-tetrahydro-1H-xanthen-1-one (LI), synthesised through the reaction of xanthene, salicylaldehyde, and ethylenediamine. The Mannich base ligand (**L1**) was used to form metal complexes (**1**– **5**) of the $[M(\mathbf{L1})_2Cl_2]$ type. These complexes were then analysed using analytical, magnetic, and spectroscopic methods. The Mannich base is a bidentate ligand that coordinates with the metal ion over nitrogen atom of ethylenediamine and the oxygen atom of salicylaldehyde. The conductivity behaviours indicate that the chloride atoms are bound to the metal atoms as ligands, rather than being as free ions. The synthesised complexes (**1–5**) exhibit the octahedral geometry as shown by their electrical and magnetic characteristics. Furthermore, the ligand and metal complexes underwent screening to evaluate their antibacterial efficacy towards different harmful microorganisms. The metal complexes displayed significant antimicrobial properties related to the ligand (**L1**) and control, as validated by docking experiments. The data acquired validate the multi-directional antimicrobial efficacy of the novel Mannich base complexes and demonstrate the influence of structural replacement on the activity of this kind of substances towards various microorganisms. The findings acquired are anticipated to yield significant data for additional study of this intriguing group. Pharmacological research focused on discovering novel biologically active chemicals is ongoing with a repository of acquired molecules.

Supporting Information

The Supporting Information is available free at https://ejc.buketov.edu.kz/index.php/ejc/article/view/232/198

*Author Information**

**The authors' names are presented in the following order: First Name, Middle Name and Last Name*

Manimegalai Ramasamy — Research Scholar, PG & Research Department of Chemistry, Government Arts College, Bharathidasan University, Ariyalur, 621713, Tamilnadu, India; e-mail: manisri627@gmail.com; https://orcid.org/0009-0002-8951-5440

Gurunathan Velayutham — Assistant Professor, PG & Research Department of Chemistry, Bishop Heber College, Bharathidasan University, Tiruchirappalli, 621002, Tamilnadu, India; e-mail: gurunathan.ch@bhc.edu.in; https://orcid.org/0009-0009-2547-5276

Ramar Pitchaipillai (*corresponding author*) — Associate Professor, PG & Research Department of Chemistry, Government Arts College, Bharathidasan University, Ariyalur, 621713, Tamilnadu, India; e-mail: drsairam202110@gmail.com; https://orcid.org/0009-0006-2022-7159

Author Contributions

The manuscript was written through contributions of all authors. All authors have given approval to the final version of the manuscript. CRediT: **Manimegalai Ramasamy** conceptualization, data curation, investigation, methodology, validation, visualization, writing-review & editing; **Gurunathan Velayutham** data curation, formal analysis, visualization; **Ramar Pitchaipillai** conceptualization, data curation, formal analysis, funding acquisition, resources, supervision, validation, writing-original draft, writing-review & editing.

Acknowledgments

The Authors are acknowledging their respective managements for giving the opportunity to accomplish this research work.

Conflicts of Interest

The authors declare no conflict of interest.

References

1 Murray C. J., Ikuta K. S., Sharara F., Swetschinski L., Robles Aguilar G., Gray A., Han C., Bisignano C., Rao P., Wool E., & Johnson S. C. (2022). Global burden of bacterial antimicrobial resistance in 2019: a systematic analysis. *Lancet*, *399*, 629–655. https://doi.org/10.1016/S0140-6736(21)02724-0

2 Cassini A., Högberg L. D., Plachouras D., Quattrocchi A., Hoxha A., Simonsen G. S., Colomb-Cotinat M., Kretzschmar M. E., Devleesschauwer B., Cecchini M., & Ouakrim D. A. (2019). Attributable deaths and disability-adjusted life-years caused by infections with antibiotic-resistant bacteria in the EU and the European Economic Area in 2015: a population-level modelling analysis. *The Lancet Infectious Diseases*, *19*, 56–66. https://doi.org/10.1016/S1473-3099(18)30605-4

3 Centers for Disease Control and Prevention US, Antibiotic Resistance Threats in the United States, https://stacks.cdc.gov/view/cdc/82532, 2019. Accessed 20th February 2025.

4 WHO: Global Antimicrobial Resistance and Use Surveillance System (GLASS) Report 2022, https://www.who.int/publications/i/item/97, 2022. Accessed 20th February 2025.

5 Darby E. M., Trampari E., Siasat P., Solsona Gaya M., Alav I., Webber M. A., & Blair J. M. A. (2022). Molecular mechanisms of antibiotic resistance revisited. *Nature Reviews Microbiology*, *21*, 280–295. https://doi.org/10.1038/s41579-022-00820-y

6 Prashanth, T., Ranganatha, V. L., Ramu, R., Mandal, S. P., Mallikarjunaswamy, C., & Khanum, S. A. (2021). Synthesis, characterization, docking study and antimicrobial activity of 2-(4-benzoylphenoxy)-1-[2-(1-methyl-1 H-indol-3-yl) methyl)-1H-benzo[d]imidazol-1-yl]ethanone derivatives. *Journal of the Iranian Chemical Society*, *18*, 2741–2756. https://doi.org/10.1007/s13738-021-02230-y

7 Khadri, M. N., Begum, A. B., Sunil, M. K., & Khanum, S. A. (2020). Synthesis, docking and biological evaluation of thiadiazole and oxadiazole derivatives as antimicrobial and antioxidant agents. *Results in Chemistry*, *2*, 100045. https://doi.org/10.1016/j.rechem.2020.100045

8 Abu-Dief, A. M., Alotaibi, N. H., Al-Farraj, E. S., Qasem, H. A., Alzahrani, S., Mahfouz, M. K., & Abdou, A. (2022). Fabrication, structural elucidation, theoretical, TD-DFT, vibrational calculation and molecular docking studies of some novel adenine imine chelates for biomedical applications. *Journal of Molecular Liquids*, *365*, 119961. https://doi.org/10.1016/j.molliq.2022.119961

9 Alatawi, N. M., Alsharief, H. H., Alharbi, A., Alhasani, M., Attar, R. M., Khalifa, M. E., ... & El-Metwaly, N. M. (2022). Simulation for the behavior of new Fe (III) and Cr (III)-thiophenyl complexes towards DNA polymerase: synthesis, characterization, eukaryotic DNA and Hartree–Fock computation. *Chemical Papers*, *76*(6), 3919–3935. https://doi.org/10.1007/s11696-022-02136-w

10 Abu-Dief, A. M., El-Khatib, R. M., Aljohani, F. S., Alzahrani, S. O., Mahran, A., Khalifa, M. E., & El-Metwaly, N. M. (2021). Synthesis and intensive characterization for novel Zn (II), Pd (II), Cr (III) and VO (II)-Schiff base complexes; DNA-interaction, DFT, drug-likeness and molecular docking studies. *Journal of Molecular Structure*, *1242*, 130693. https://doi.org/10.1016/j.molstruc.2021.130693

11 Abu-Dief, A. M., Abdel-Rahman, L. H., Abdelhamid, A. A., Marzouk, A. A., Shehata, M. R., Bakheet, M. A., ... & Nafady, A. (2020). Synthesis and characterization of new Cr (III), Fe (III) and Cu (II) complexes incorporating multi-substituted aryl imidazole ligand: Structural, DFT, DNA binding, and biological implications. *Spectrochimica Acta Part A: Molecular and Biomolecular Spectroscopy*, *228*, 117700. https://doi.org/10.1016/j.saa.2019.117700

12 Abdel-Rahman, L. H., Abu-Dief, A. M., El-Khatib, R. M., & Abdel-Fatah, S. M. (2016). Sonochemical synthesis, DNA binding, antimicrobial evaluation and in vitro anticancer activity of three new nano-sized Cu (II), Co (II) and Ni (II) chelates based on tridentate NOO imine ligands as precursors for metal oxides. *Journal of Photochemistry and Photobiology B: Biology*, *162*, 298–308. https://doi.org/10.1016/j.jphotobiol.2016.06.052

13 Khalaf, M. M., Abd El-Lateef, H. M., Gouda, M., Sayed, F. N., Mohamed, G. G., & Abu-Dief, A. M. (2022). Design, structural inspection and bio-medicinal applications of some novel imine metal complexes based on acetylferrocene. *Materials*, *15*(14), 4842. https://doi.org/10.3390/ma15144842

14 Abu-Dief, A. M., El-Khatib, R. M., Aljohani, F. S., Al-Abdulkarim, H. A., Alzahrani, S., El-Sarrag, G., & Ismael, M. (2022). Synthesis, structural elucidation, DFT calculation, biological studies and DNA interaction of some aryl hydrazone Cr^{3+}, Fe^{3+}, and Cu^{2+} chelates. *Computational Biology and Chemistry*, *97*, 107643. https://doi.org/10.1016/j.compbiolchem.2022.107643

15 Borah, B., Dwivedi, K. D., & Chowhan, L. R. (2021). Recent advances in metal-and organocatalyzed asymmetric functionalization of pyrroles. *Asian Journal of Organic Chemistry*, *10*(11), 2709–2762. https://doi.org/10.1002/ajoc.202100427

16 Borah, B., Dhar Dwivedi, K., & Chowhan, L. R. (2021). 4-Hydroxycoumarin: A versatile substrate for transition-metal-free multicomponent synthesis of bioactive heterocycles. *Asian Journal of Organic Chemistry*, *10*(12), 3101–3126. https://doi.org/10.1002/ajoc.202100550

17 Mermer, A., Keles, T., & Sirin, Y. (2021). Recent studies of nitrogen containing heterocyclic compounds as novel antiviral agents: A review. *Bioorganic Chemistry*, *114*, 105076. https://doi.org/10.1016/j.bioorg.2021.105076

18 Azath, I. A., Puthiaraj, P., & Pitchumani, K. (2013). One-pot multicomponent solvent-free synthesis of 2-amino-4H-benzo [b]pyrans catalyzed by per-6-amino-β-cyclodextrin. *ACS Sustainable Chemistry & Engineering*, *1*(1), 174–179. https://doi.org/10.1021/sc3000866

19 Datta, B., & Pasha, M. A. (2012). Glycine catalyzed convenient synthesis of 2-amino-4H-chromenes in aqueous medium under sonic condition. *Ultrasonics Sonochemistry*, *19*(4), 725–728. https://doi.org/10.1016/j.ultsonch.2012.01.006

20 Gourdeau, H., Leblond, L., Hamelin, B., Desputeau, C., Dong, K., Kianicka, I., ... & Tseng, B. (2004). Antivascular and antitumor evaluation of 2-amino-4-(3-bromo-4, 5-dimethoxy-phenyl)-3-cyano-4H-chromenes, a novel series of anticancer agents. *Molecular cancer therapeutics*, *3*(11), 1375–1384. https://doi.org/10.1158/1535-7163.1375.3.11

21 Kemnitzer, W., Drewe, J., Jiang, S., Zhang, H., Wang, Y., Zhao, J., ... & Cai, S. X. (2004). Discovery of 4-Aryl-4 H-chromenes as a new series of apoptosis inducers using a cell-and caspase-based high-throughput screening assay. 1. structure− activity relationships of the 4-Aryl group. *Journal of medicinal chemistry*, *47*(25), 6299–6310. https://doi.org/10.1021/jm049640t

22 Mohr, S. J., Chirigos, M. A., Fuhrman, F. S., & Pryor, J. W. (1975). Pyran copolymer as an effective adjuvant to chemotherapy against a murine leukemia and solid tumor. *Cancer research*, *35*(12), 3750–3754.

23 Hatakeyama, S., Ochi, N., Numata, H., & Takano, S. (1988). A new route to substituted 3-methoxycarbonyldihydropyrans; enantioselective synthesis of (–)-methyl elenolate. *Journal of the Chemical Society, Chemical Communications*, (17), 1202–1204. https://doi.org/10.1039/C39880001202

24 Bonsignore, L., Loy, G., Secci, D., & Calignano, A. (1993). Synthesis and pharmacological activity of 2-oxo-(2H)-1-benzopyran-3-carboxamide derivatives. *European Journal of Medicinal Chemistry*, *28*(6), 517–520. https://doi.org/10.1016/0223-5234(93)90020-F

25 Görlitzer, K., Dehne, A., & Engler, E. (1983). 2-(1H-Tetrazol-5-yl)-4,5-dihydro-4-oxo-indeno[1,2-b]pyran. *Archiv der Pharmazie*, *316*(3), 264–270. https://doi.org/10.1002/ardp.19833160315

26 Alvey, L., Prado, S., Huteau, V., Saint-Joanis, B., Michel, S., Koch, M., ... & Janin, Y. L. (2008). A new synthetic access to furo[3,2-f]chromene analogues of an antimycobacterial. *Bioorganic & medicinal chemistry*, *16*(17), 8264–8272. https://doi.org/10.1016/j.bmc.2008.06.057

27 Kumar, R. R., Perumal, S., Senthilkumar, P., Yogeeswari, P., & Sriram, D. (2007). An atom efficient, solvent-free, green synthesis and antimycobacterial evaluation of 2-amino-6-methyl-4-aryl-8-[(E)-arylmethylidene]-5,6,7,8-tetrahydro-4H-pyrano[3,2-c]pyridine-3-carbonitriles. *Bioorganic & Medicinal Chemistry Letters*, *17*(23), 6459–6462. https://doi.org/10.1016/j.bmcl.2007.09.095

28 Armesto, D., Horspool, W. M., Martin, N., Ramos, A., & Seoane, C. (1989). Synthesis of cyclobutenes by the novel photochemical ring contraction of 4-substituted 2-amino-3, 5-dicyano-6-phenyl-4H-pyrans. *The Journal of Organic Chemistry*, *54*(13), 3069–3072. https://doi.org/10.1021/jo00274a021

29 Reynolds, G. A., & Drexhage, K. H. (1975). New coumarin dyes with rigidized structure for flashlamp-pumped dye lasers. *Optics Communications*, *13*(3), 222–225. https://doi.org/10.1016/0030-4018(75)90085-1

30 Azizi, N., Mariami, M., & Edrisi, M. (2014). Greener construction of 4H-chromenes based dyes in deep eutectic solvent. *Dyes and Pigments*, *100*, 215–221. https://doi.org/10.1016/j.dyepig.2013.09.007

31 Bissell, E. R., Mitchell, A. R., & Smith, R. E. (1980). Synthesis and chemistry of 7-amino-4-(trifluoromethyl) coumarin and its amino acid and peptide derivatives. *The Journal of Organic Chemistry*, *45*(12), 2283–2287. https://doi.org/10.1021/jo01300a003

32 Ellis, G.P. Chromenes, Chromanones, and Chromones—Introduction. *Chemistry of Heterocyclic Compounds*, 1–10. Portico. https://doi.org/10.1002/9780470187012.ch1

33 Singha, R., Islam, A., & Ghosh, P. (2021). One-pot three-component tandem annulation of 4-hydroxycoumarine with aldehyde and aromatic amines using graphene oxide as an efficient catalyst. *Scientific Reports*, *11*(1), 19891. https://doi.org/10.1038/s41598-021-99360-3

34 Bui, T. H., Le, T. T., Vu, T. T., Hoang, X. T., Luu, V. C., Vu, D. H., & Tran, K. V. (2012). Design, synthesis and in vitro cytotoxic activity evaluation of new Mannich bases. *Bulletin of the Korean Chemical Society*, *33*(5), 1586–1592. http://dx.doi.org/10.5012/bkcs.2012.33.5.1586

35 Arend, M., Westermann, B., & Risch, N. (1998). Modern variants of the Mannich reaction. *Angewandte Chemie International Edition*, *37*(8), 1044–1070. https://doi.org/10.1002/(SICI)1521-3773

36 Kobayashi, S., & Ueno, M. (2004). Comprehensive asymmetric catalysis. In Comprehensive Asymmetric Catalysis (p. 143). Springer.

37 Blicke, F. F. (1942). The Mannich Reaction; Organic Reactions; John Wiley & Sons, Hoboken, New Jersey, United States, 303–341.

38 Ramón, D. J., & Yus, M. (2005). Asymmetric multicomponent reactions (AMCRs): the new frontier. *Angewandte Chemie International Edition*, *44*(11), 1602–1634. https://doi.org/10.1002/anie.200460548

39 Jayabalakrishnan, C., & Natarajan, K. (2001). Synthesis, characterization, and biological activities of ruthenium (II) carbonyl complexes containing bifunctional tridentate Schiff bases. *Synthesis and Reactivity in Inorganic and Metal-Organic Chemistry*, *31*(6), 983–995. https://doi.org/10.1081/SIM-100105255

40 Jeewoth, T., Li Kam Wah, H., Bhowon, M. G., Ghoorohoo, D., & Babooram, K. (2000). Synthesis and antibacterial/catalytic properties of Schiff bases and Schiff base metal complexes derived from 2,3-diaminopyridine. *Sythesis and Reactivity in Inorganic and Matel-Organic Chemistry*, *30*(6), 1023–1038. https://doi.org/10.1080/00945710009351817

41 List, B. (2000). The direct catalytic asymmetric three-component Mannich reaction. *Journal of the American Chemical Society*, *122*(38), 9336–9337. https://doi.org/10.1021/ja001923x

42 Eftekhari-Sis, B., Abdollahifar, A., Hashemi, M. M., & Zirak, M. (2006). Stereoselective Synthesis of β-Amino Ketones via Direct Mannich-Type Reactions, Catalyzed with $ZrOCl_2 \cdot 8H_2O$ under Solvent-Free Conditions. *European Journal of Organic Chemistry*, *2006(22)*, 5152–5157. https://doi.org/10.1002/ejoc.200600493

43 Mitsumori, S., Zhang, H., Ha-Yeon Cheong, P., Houk, K. N., Tanaka, F., & Barbas, C. F. (2006). Direct Asymmetric a nti-Mannich-Type Reactions Catalyzed by a Designed Amino Acid. *Journal of the American Chemical Society*, *128*(4), 1040–1041. https://doi.org/10.1021/ja056984f

44 Al-Jeboori, M. J., Al-Jebouri, F. A., & Al-Azzawi, M. A. (2011). Metal complexes of a new class of polydentate Mannich bases: Synthesis and spectroscopic characterisation. *Inorganica Chimica Acta*, *379*(1), 163–170. https://doi.org/10.1016/j.ica.2011.10.013

45 Fernández-Fariña S., Velo-Heleno I., Martínez-Calvo M., González-Noya A. M., & Pedrido R. (2022). Design, synthesis and structural characterization of a novel asymmetric hydrazone-thiosemicarbazone ligand with the aim of obtaining ınteresting metallosupramolecular architectures. *Chemistry Proceedings*, *8*, 16. https://doi.org/10.3390/ecsoc-25-11738

46 Kirtani D. U., Ghatpande N. S., Suryavanshi K. R., Kulkarni P. P., & Kumbhar A. A. (2021). Fluorescent copper(II) complexes of asymmetric bis(thiosemicarbazone)s: Electrochemistry, cellular uptake and antiproliferative activity. *Chemistry Select*, *6*, 6063–6070. https://doi.org/10.1002/slct.202101663

47 Özdemir N., Şahin M., Bal-Demirci T., & Ülküseven B. (2011). The asymmetric ONNO complexes of dioxouranium(VI) with N1, N4-diarylidene-S-propyl-thiosemicarbazones derived from 3,5-dichlorosalicylaldehyde: Synthesis, spectroscopic and structural studies. *Polyhedron*, *30*, 515–521. https://doi.org/10.1016/j.poly.2010.11.030

48 Varadinova T., Kovala-Demertzi D., Rupelieva M., Demertzis M., & Genova P. (2001). Antiviral activity of platinum (II) and palladium (II) complexes of pyridine-2-carbaldehyde thiosemicarbazone. *Acta Virologica*, *45*, 87–94.

49 Pandeya S. N., & Dimmock J. R. (1993). Recent evaluations of thiosemicarbazones and semicarbazones and related compounds for antineoplastic and anticonvulsant activities, *Die Pharmazie*, 1993, *48*, 659–666.

50 Bauer, A. W., Kirby, W. M. M., Sherris, J. C., & Turck, M. (1966). Antibiotic susceptibility testing by a standardized single disk method. *American journal of clinical pathology*, *45*, 493–496. https://doi.org/10.1093/ajcp/45.4_ts.493

51 Ferrari, M. B., Capacchi, S., Pelosi, G., Reffo, G., Tarasconi, P., Albertini, R., ... & Lunghi, P. (1999). Synthesis, structural characterization and biological activity of helicin thiosemicarbazone monohydrate and a copper (II) complex of salicylaldehyde thiosemicarbazone. *Inorganica Chimica Acta*, *286*(2), 134–141. https://doi.org/10.1016/S0020-1693(98)00383-1

52 Abd El-Wahab, Z. H., Mashaly, M. M., Salman, A. A., El-Shetary, B. A., & Faheim, A. A. (2004). Co (II), Ce (III) and UO_2 (VI) bis-salicylatothiosemicarbazide complexes: binary and ternary complexes, thermal studies and antimicrobial activity. *Spectrochimica Acta Part A: Molecular and Biomolecular Spectroscopy*, *60*(12), 2861–2873. https://doi.org/10.1016/j.saa.2004.01.021

53 Wallingford, V. H., & Krueger, P. A. (1939). 5-iodoanthranilic acid. *Organic Synthesis*, *19*, 52.

54 Bauer, A. W., Kirby, W. M. M., Sherris, J. C., & Turck, M. (1966). Antibiotic susceptibility testing by a standardized single disk method. *American journal of clinical pathology*, *45*(4_ts), 493–496. https://doi.org/10.1093/ajcp/45.4_ts.493

55 Trott, O., & Olson, A. J. (2010). AutoDock Vina: improving the speed and accuracy of docking with a new scoring function, efficient optimization, and multithreading. *Journal of computational chemistry*, *31*(2), 455–461. https://doi.org/10.1002/jcc.21334

56 Al-Dobony, B. S., & Al-Assafe, A. Y. (2019). Synthesis, characterization and antimicrobial studies of some metal complexes with mixed ligands derived from Mannich bases and diamine ligands. *Journal of Physics: Conference Series, 1294*(5), 052068. https://doi.org/10.1088/1742-6596/1294/5/052068

57 Balakrishnan, A. & Sankar, A. (2016) Studies on the synthesis and characterization of the transition metal complexes of novel mannich base. *International Journal of Pharmaceutical, Chemical & Biological Sciences*, *6*, 150.

58 Raman, N., Malaramani, R.V., & Thangaraja, C. (2004). Synthesis and physico-chemical characterization of a new Mannich base, N(morpholinobenzyl)benzamide and its Cu(Il), Co(ll), Ni(II) and Zn(Il) complexes. *Indian Journal of Chemistry*, *43A*, 2357–2360.

59 Janowska, S., Andrzejczuk, S., Gawryś, P. & Wujec, M. (2023). Synthesis and Antimicrobial Activity of New Mannich Bases with Piperazine Moiety. *Molecules*, *28*, 562. https://doi.org/10.3390/molecules28145562

60 Tamilvendan, D., Rajeswari, S., Ilavenil, S., Chakkaravarthy, K., & Venkatesa Prabhu, G. (2012). Syntheses, spectral, crystallographic, antimicrobial, and antioxidant studies of few Mannich bases. *Medicinal Chemistry Research*, *21*, 4129–4138. https://doi.org/10.1007/s00044-011-9944-2

61 Selvaraj, S.D., Krishnaveni, R., & Tamilvendan, D. (2020). Synthesis, characterization, anticorrosion and antimicrobial studies of novel 1-[anilino (phenyl)methyl]pyrimidine-2,4,6-trione derived from Mannich reaction and its metal complexes. *Materials Today: Proceedings*, *33*, 4271–4279. https://doi.org/10.1016/j.matpr.2020.07.400

62 Singh, V., Praveen, V., Tripathi, D., Haque, S., Somvanshi, P., Katti, S. B., & Tripathi, C. K. M. (2015). Isolation, characterization and antifungal docking studies of wortmannin isolated from Penicillium radicum. *Scientific reports*, *5*(1), 11948. https://doi.org/10.1038/srep11948

63 Gullapelli, K., Brahmeshwari, G., Ravichander, M., & Kusuma, U. (2017). Synthesis, antibacterial and molecular docking studies of new benzimidazole derivatives. *Egyptian journal of basic and applied sciences*, *4*(4), 303–309. https://doi.org/10.1016/j.ejbas.2017.09.002

64 Ali, D., Alarifi, S., Chidambaram, S. K., Radhakrishnan, S. K., & Akbar, I. (2020). Antimicrobial activity of novel 5-benzylidene-3-(3-phenylallylideneamino) imidazolidine-2,4-dione derivatives causing clinical pathogens: Synthesis and molecular docking studies. *Journal of Infection and Public Health*, *13*(12), 1951–1960. https://doi.org/10.1016/j.jiph.2020.09.017

65 Taha, M., Ismail, N. H., Khan, A., Shah, S. A. A., Anwar, A., Halim, S. A., ... & Khan, K. M. (2015). Synthesis of novel derivatives of oxindole, their urease inhibition and molecular docking studies. *Bioorganic & Medicinal Chemistry Letters*, *25*(16), 3285–3289. https://doi.org/10.1016/j.bmcl.2015.05.069